



Title	Structural Optimization Final Technical Report		
Document No.	DE-EE0006610 M6.1 Final Report		
Version	2.0		
Prime Contract	DE-EE0006610		
Authored	Pukha Lenee-Bluhm		
Reviewed	Michael Ondusko, Reenst Lesemann, Brad Lamb		
Version Approved			
Data Classification	<input type="checkbox"/> Limited Rights Data	<input type="checkbox"/> Protected Data	<input checked="" type="checkbox"/> Unlimited Data

Version	Date	Summary
1.0	11/27/19	Release with Final Reporting
2.0	08/05/20	Requested Clarification

Acknowledgement: The information, data, or work presented herein was funded in part by the U.S. Department of Energy's Office of Energy Efficiency and Renewable Energy (EERE), Water Power Technologies Office, under Award Number DE-EE0006610.

The information, data, or work presented herein was funded in part by an *agency* of the United States Government. Neither the United States Government nor any agency thereof, nor any of their employees, makes any warranty, express or implied, or assumes any legal liability or responsibility for the accuracy, completeness, or usefulness of any information, apparatus, product, or process disclosed, or represents that its use would not infringe privately owned rights. Reference herein to any specific commercial product, process, or service by trade name, trademark, manufacturer, or otherwise does not necessarily constitute or imply its endorsement, recommendation, or favoring by the United States Government or any agency thereof. The views and opinions of authors expressed herein do not necessarily state or reflect those of.

TABLE OF CONTENTS

1	EXECUTIVE SUMMARY	1
2	LIST(S) OF SYMBOLS, ABBREVIATIONS, AND ACRONYMS	1
3	INTRODUCTION.....	4
4	NEXT-GENERATION HULL ARCHITECTURE DESIGN.....	5
4.1	Next-generation Hull Concept	5
4.2	Design Loads	5
4.3	Structural analysis and design.....	7
4.4	Geometric Areas of Interest for Further Optimization	9
5	TEST-SUPPORTED MIXED MATERIALS OPTIMIZATION	11
5.1	Mixed Materials Concept.....	11
5.2	Laboratory Testing	12
5.3	Mixed Materials Optimization	16
6	PROJECT IMPROVEMENTS AND IMPACT	22
6.1	Next-Generation WEC Hull	22
6.2	Test-Supported Mixed Materials Optimization	22
6.3	SPA and LCOE Impact.....	23
7	CHALLENGES AND LESSONS LEARNED.....	24
8	SYSTEM INTEGRATION AND FUTURE WORK	25
9	CONCLUSIONS.....	25
10	REFERENCES.....	27
11	APPENDICES [PROTECTED DATA]	28
11.1	Appendix: Design Load Cases for Structural Optimization	28
11.2	Appendix: Metocean Report.....	28
11.3	Appendix: StingRAY Design Loads.....	28
11.4	Appendix: CPower WEC Design Documentation	28
11.5	Appendix: CPower WEC Structural Arrangement.....	28
11.6	Appendix: Summary of Component Design Report.....	28
11.7	Appendix: Test Article Design Technical Memo	28
11.8	Appendix: Composite Test Program Memo.....	28
11.9	Appendix: WEC Design Alternative Composites Coupon Panels	28
11.10	Appendix: CPower Coupon and Double Lap Shear Specimen Test Report (public data)	28
11.11	Appendix: Optimization Memo.....	28
11.12	Appendix: SPA and LCOE Impact Assessment.....	28
11.13	Appendix: Energy Production Assessment for DOE LCOE and SPA Reporting.....	28
11.14	Appendix: Baseline and Final TAEP Calculations.....	28

11.15	Appendix: System Integration Plan.....	29
-------	--	----

TABLE OF FIGURES

Figure 1 – Criteria for selection of geometric areas of interest for further optimization.	10
Figure 2 – Double lap shear joint concept detail.	11
Figure 3 – Filament winding mold, and helical winding process.	14
Figure 4 – Steel and composite coupons prior to assembly into DLS specimens.	15
Figure 5 – DLS specimen curing in fixture (left), and five cured DLS specimens (right).	15
Figure 6 – Tsai Wu Failure Criteria for slamming load case.	18
Figure 7 – Typical double lap shear static testing failure.	19
Figure 8 – Fatigue data and SN curves for 0.5 in. Plexus MA560 and Araldite 2013.	21

TABLE OF TABLES

Table 1 – Symbols, Abbreviations, and Acronyms	1
Table 2 – Material properties determined from filament wound (FW) coupons.	17
Table 3 – Material properties determined from uniaxial (UNI) coupons.	17
Table 4 – Thickness, density, and FVF for FW and UNI materials.	17
Table 5 – Characteristic shear strength of double lap shear joints.	20
Table 6 – Targeted system improvements goals.	23
Table 7 – Targeted and actual SPA metric and LCOE improvements.	23

1 EXECUTIVE SUMMARY

Columbia Power Technologies, Inc. (C-Power) is developing a direct drive, rotary (DDR) wave energy converter (WEC) for utility-scale power applications, known as the StingRAY. The DE-EE0006610 (6610) Project objectives were to improve the overall Power-to-Weight Ratio (PWR) and decrease Levelized Cost of Energy (LCOE) of the StingRAY. This was achieved by decreasing capital expenditures (CAPEX), reducing structural mass, and increasing energy production performance.

A major redesign of the baseline StingRAY (H1) WEC hull structure was completed under this Project. This next-generation StingRAY (H2) WEC hull architecture significantly increases power performance, while reducing complexity and cost of the WEC system through efficient use of structural and power generation components, along with simplified component geometries aimed at reducing manufacturing costs. The H2 design was progressed from concept to final design with structural drawings, in preparation for a planned deployment at the Wave Energy Test Site (WETS) offshore of the Marine Corp Base Hawaii (MCBH) in Kaneohe Bay.

A mixed materials approach to further structural optimization was developed under this Project and validated with extensive laboratory structural testing. This approach substitutes fiber-reinforced plastic (FRP) for steel where appropriate. The benefits of steel are maintained where most useful, for instance at structural joints where the stiffness of steel is required, and the complex geometry is more readily fabricated with steel. However, there are structural spans whose simple shapes are readily fabricated with mandrel-wound FRP and where significant cost and weight savings can be found. An adhesive, double lap shear joint is used to join the FRP and steel subcomponents.

Extensive coupon testing was conducted to assess constituent material properties of the as-built FRP laminate, allowing for the design layout to be optimized. Test specimens representing full-scale sections of the adhesive joint were fabricated and tested under ultimate and fatigue loading conditions. The results indicated that at least two of the tested adhesives satisfied all design requirements, validating the feasibility of the mixed materials design concept. The data sets generated from coupon and adhesive joint specimen testing will be provided to Sandia National Laboratory will be made available publicly on the MHK database, benefitting industry generally.

The Project system performance assessment (SPA) metric improvement goals were substantially surpassed, with H2 improvements relative to H1 of 99.4% and 88.0% for Active Weight (AW) and Dry Weight (DW) PWR, respectively. Although there was no specific goal established for LCOE improvement, the 54.1% reduction relative to H1 represents a resounding success for the Project. The design advancements realized under this Project materially progress C-Power's renewable energy WEC technology towards commercialization, used as the basis for Installation Operation & Maintenance improvements developed in a later DOE-funded project.

2 LIST(S) OF SYMBOLS, ABBREVIATIONS, AND ACRONYMS

Table 1 – Symbols, Abbreviations, and Acronyms

5930 ¹	DE-EE0005930 - Direct Drive Wave Energy Buoy
6399 ¹	DE-EE0006399 - Build and Test of a Novel, Commercial-Scale Wave Energy Direct-Drive

¹ Project Product was leveraged in DE-EE0006610 Wave Energy Converter Structural Optimization through Engineering and Experimental Analysis.

	Rotary Power-Take-Off Under Realistic Open-Ocean Conditions
6610 ²	DE-EE0006610 - Wave Energy Converter Structural Optimization through Engineering and Experimental Analysis
7347 ³	DE-EE0007347 - Reduction of System Cost Characteristics Through Innovative Solutions to Installation, Operations, and Maintenance
8954 ³	DE-EE0008954 - Optimization, design, and commercialization planning of next-generation StingRAY H3 Wave Energy Converter
AEP	Annual Energy Production
ASTM	American Society for Testing Materials
AW	Active Weight
C-Power	Columbia Power Technologies, Inc.
CAPEX	Capital Expense
CCI	Corrosion Companies, Inc.
CLC	Combined Loading Compression
CSM	Chapped Strand Matt
DDR	Direct Drive Rotary
DLC	Design Load Cases
DLS	Double Lap Shear
DOF	Degree(s) of Freedom
DW	Dry Weight
FEA	Finite Element Analysis
FMECA	Failure Mode, Effects and Criticality Analysis
FOA	Funding Opportunity Announcement
FRP	Fiber Reinforced Plastic
FVF	Fiber Volume Fraction
FW	Filament-wound
GAI	General Areas of Interest
Glostén	Glostén, Inc.
H1	StingRAY (Baseline)
H2	StingRAY (WETS)
H3	StingRAY (Next generation)
LCOE	Levelized Cost of Energy
LFRD	Load and Resistance Factor Design
MCBH	Marine Corps Base Hawaii
NREL	National Renewable Energy Laboratory
NWTC	National Wind Technology Center
PSF	Partial Safety Factor

² DE-EE0006610 - Wave Energy Converter Structural Optimization through Engineering and Experimental Analysis leveraged the Project Product from Projects 5930 and 6399.

³ DE-EE0007347 and DE-EE0008954 both leverage the Project Product of this Project, 6610.

PTO	Power Take-Off
PWR	Power-to-Weight Ratio
QUAD	Quadraxial fabric
SBV	Small Business Venture
SCF	Stress Concentration Factor
SOPO	Statement of Project Objectives
SPA	System Performance Advancement
TWFC	Tsai-Wu Failure Criterion
UNI	Uniaxial
UTM	Universal Test Machine
WEC	Wave Energy Converters
WETS	Wave Energy Test Site

3 INTRODUCTION

Columbia Power Technologies, Inc. (C-Power) is developing a direct drive, rotary (DDR) wave energy converter (WEC) for utility-scale power applications, known as the StingRAY. The DE-EE0006610 (6610) Project objectives were to improve the overall Power-to-Weight Ratio (PWR) and decrease Levelized Cost of Energy (LCOE). This was achieved by decreasing capital expenditures (CAPEX), reducing structural mass, and increasing energy production performance.

The purpose of this report is to summarize the technical accomplishments achieved as a result of Project efforts. There were two primary efforts within the Project. The first was a transformation of the WEC hull architecture, beginning with a concept and ending with a final design with structural drawings. The second effort was a laboratory test-supported investigation into a mixed materials concept aimed at further optimization of the hull structure.

The transformation from the 6610 Project Baseline (H1) StingRAY WEC architecture to next-generation (H2) StingRAY hull design is summarized in Section 4. This effort began with a new hull architecture concept, developed in conjunction with a cost reduction examination within DE-EE0007347 (7347), that aimed to utilize materials and components more efficiently than the Baseline hull. Engineering design requirements and design loads were then developed, and a rigorously applied design methodology resulted in a hull design suitable for the prototype deployment planned for the Wave Energy Test Site (WETS) at Marine Corp Base Hawaii (MCBH) in Kaneohe Bay. This new hull design used less costly ballast than the Baseline WEC and can produce more energy with comparable active or dry mass.

While the all-steel hull design was appropriate for the prototype deployment it was intended for, additional structural optimization through the use of mixed materials was pursued as the second major effort of this Project and is summarized in Section 5. To reduce structural cost and weight, a proposal was made to substitute FRP for steel where appropriate. A test program was developed to assess material properties of the FRP constituents, allowing for optimization of the laminate, and to assess candidate adhesives for the proposed steel-to-FRP adhesive bonds. The potential for cost and weight reduction from this hybrid steel-FRP concept was assessed.

Project improvements are summarized in Section 6, and the impact on Project Objectives is quantified using System Performance Assessment (SPA) metrics. To meet Marine Hydrokinetic SPA Goal 1 from the Funding Opportunity Announcement, the Project improvements must result in an increase in AW PWR of 64%, and an increase in DW PWR of 15%. SPA metric improvement goals were substantially surpassed, with H2 improvements relative to H1 of 99.4% and 88.0% for Active Weight (AW) and Dry Weight (DW) PWR, respectively.

Challenges and lessons learned are discussed in Section 7. System integration and future work are discussed in Section 8. Project conclusions are summarized in Section 9 and references are listed in Section 10. Additional detailed reporting is provided as Appendices in Section 11; while this report body is public, the Appendices are all marked “Protected Data” with the exception of the *Test Report* provided as Appendix 11.10.

Note that due to the proprietary nature of the next-generation H2 WEC design, no descriptive details regarding the design are contained in the public version of this report. Such details are restricted to the “Protected Data” Appendices.

4 NEXT-GENERATION HULL ARCHITECTURE DESIGN

4.1 Next-generation Hull Concept

C-Power developed the StingRAY under grant DE-EE0005930 (FOA0293). The StingRAY v3.1, later renamed StingRAY H1. This design was a three-body point absorber with two floats operating two independent PTO/generators. StingRAY H2 was conceived to improve upon the H1 design. In alignment with the 6610 Project objectives and a desire to capitalize on technical advancements, DOE and C-Power agreed that the improved H2 WEC architecture should be integrated with the 6610 Project. Under 6610, the H2 WEC was progressed from concept to final design with structural drawings, and a mixed materials approach to further structural optimization was validated with extensive laboratory structural testing. The Project Baseline WEC is the H1, and the Project Final WEC is a mixed materials H2. The revised architecture has numerous benefits including lower part count, more efficient use of materials, lower-cost ballast, and increased power performance.

The design requirements included a five-year design life at MCBH WETS.. Additional requirements included the ability to float in both power production and shallow-draft towing configurations without the use of additional buoyancy components, and internal compartmenting to reduce the risk of sinking in the event of a hull breach.

The scope of the Project design comprised the hull structure, along with structural features for interfacing with the power take-off (PTO) system; attachment points for mooring, lifting, and towing; and ballasting for transport, towing, and power production operations.

4.2 Design Loads

4.2.1 Design load cases

A detailed assessment of WEC loading was critical for the requisite structural analysis. Specification of the design load cases (DLCs) was guided by *IEC 62600-2 Design requirements for marine energy systems* [1]. Detailed description of the DLCs, and justification of their selection, is covered in *M2.1-Design Load Cases for Structural Optimization* (Appendix 11.1).

Normal and extreme conditions of the design environment, WETS test Berth B, were encompassed by the DLCs. The WETS berth is at 80 m water depth, and C-Power characterization of the metocean conditions is described in *Metocean Report S1-DB-01* (Appendix 11.2). A subset of 24 sea states was selected to represent the normal wave conditions. The 50-year return storm represents the extreme wave conditions. Wind, current, and tidal conditions were not considered significant to the design considering the low profile of the WEC, the low current speeds of the design environment, and the compliant mooring.

All phases of the WEC lifecycle were considered in the DLCs, including fabrication, transportation, towing, deployment, and power production operations. In addition to normal operation (no faults), consideration was given to fault states, damaged stability, and other potential events.

A Failure Mode, Effects and Criticality Analysis (FMECA) was performed by C-Power [2] and was used to guide DLC specification. One critical issue identified from the FMECA was that system faults lead to a freewheeling PTO. Grid loss leads to *islanding mode* in which the generator damping is very light such that only station power is produced (this small amount of damping is not significantly different from freewheeling). It is possible for faults to lead to reduced generator damping, but normal generator control and freewheeling were investigated and there was no need to also analyze an intermediate state.

The DLCs were assessed for design criticality, and were categorized as critical, optional, or insignificant. The critical DLCs were determined to be power production in normal seas; extreme seas; and freewheeling in extreme seas.

4.2.2 Time series of loading from hydrodynamic simulations

Loads were assessed computationally using fully-coupled time-domain numerical simulations, accounting for all load contributions simultaneously (ANSYS AQWA-NAUT v16). All relevant loads were considered in the calculations, including hydrodynamic loading, inertial loading, and functional loading from PTO and mooring. The hydrodynamic loads included hydrostatic, Froude-Krylov, viscous drag, added mass, and drift forces.

The WEC was decomposed and modeled as N substructures, with substructures connected either rigidly or via single degree of freedom (DOF) hinged joint as appropriate. The decomposition allowed for AQWA to output N separate sets of loading time series. Thus, for each DLC simulated there was a time series of hydrodynamic loading, acceleration, velocity, depth, and body-to-body constraint loads for each of N substructures; generator torque; PTO friction and non-torque constraint loading; and mooring and umbilical attachment point loading. In extreme seas, some substructures occasionally left and re-entered the water. In these instances, a slamming pressure was estimated from concurrent hydrodynamic loads and wetted surface areas.

Details of model set up, and description of loads and other outputs, are given in *SR-Design Loads* (Appendix 11.3).

Ten 3-hour simulations were run for power production mode in extreme seas, and another ten 3-hour simulations for freewheeling in extreme seas. Each simulation had a unique set of random phase angles for the spectral components. The seas were modeled with directional spreading, but with the mean direction head-on to the WEC (as the single-point mooring allows the WEC to align itself with the waves). Two additional 3-hour simulations were run for a bimodal extreme sea, one in power production mode and one freewheeling. The bidirectional sea state had the same overall significant wave height and energy period but split the waves into separate wind and swell components, that were separated directionally by 90°. The normal wave conditions were not simulated (see 4.3.4 for details on fatigue assessment). All simulations were run with 0.0111 second time step (90 Hz), to fully capture the dynamics of the wave-induced loading. To keep files sizes manageable for structural analysis the resulting time series outputs were down-sampled by a factor of ten.

4.2.3 Structural design loads

A finite element analysis (FEA) was utilized to assess design loads for each of the substructures (see *CPower WEC Design Documentation* in Appendix 11.4 for details). To reduce the computational load, first the 3-hour simulations were pre-screened to select four 3-hour worst-case simulations for both the power production and the freewheeling cases. The pre-screening criteria considered maximum body motions along with maximum body-to-body constraint loads (joint loads). A total of ten simulations (four power production, four freewheeling, and both bidirectional cases) were selected.

The ten pre-screened cases were evaluated with FEA at every other time step (to keep file sizes manageable it was necessary to down-sample the time series inputs by a factor of two). The finite element model was created in Nx Nastran using massless beam elements with cylindrical tube sections. The analysis assumed unstiffened cross sections with rule minimum thicknesses for the tube walls in order to approximate the relative stiffness between members. The mass of each structural element was modeled as a point mass located at the center of gravity. Each load case was dynamically balanced with the calculated acceleration and velocities from the simulation time step. Functional loads from the PTO, mooring, and umbilical were applied.

The FEA results were post-processed to identify the maximum and minimum bending moment, axial force, shear, and torsion in each of the N substructures. The original intent of the ten simulations was to provide data for statistical evaluation of the loads. This approach was abandoned in favor of providing concurrent

balanced load sets for structural design that maximize each process of interest. The results indicate that the bidirectional cases govern for many load processes, so a statistical approach is not possible in those cases and the adopted approach lends consistency.

The maximum local design pressures from depth and slamming were taken directly from the post-processing of the AQWA simulations. These loads were not included in the FEA, but they were included as loads in the design calculations.

4.3 Structural analysis and design

Glosten, a naval architecture firm, was contracted to perform the structural analysis and design. Structural analysis and design are covered in detail in *CPower WEC Design Documentation* in Appendix 11.4. The structural arrangement is provided in Appendix 11.5.

4.3.1 Shells

The WEC is a fabricated steel structure formed by a combination of cylindrical shell structures. Each cylindrical shell member of the WEC was analyzed in accordance with the Load and Resistance Factor Design (LFRD) method outlined in *DNV-OS-C101 Design of Offshore Steel Structures* [3].

Eight independent load cases were considered for each major cylindrical shell substructure. Six of these cases were taken from the FEA described above (see 4.2.3) and comprised the maximum load in each DOF and the concurrent loads from that time step. A partial safety factor (PSF) of 1.35 was applied to these loads as recommended by *IEC 62600-2* [1]. The other two cases considered external and internal pressure: hydrostatic pressure from depth and compressed air used for purging the variable seawater ballast. A PSF of 1.2 was applied to these loads as recommended by *DNV-OS-C101* [3].

The global stresses were derived from formulae for stresses in closed cylinders per *DNV-RP-C202 Buckling Strength of Shells* [4]. In general, the material PSF was 1.15 as per *IEC 62600-2* [1]. All shell plating was assumed to be NV AH36 steel (equivalent to ABS AH36) in an effort to reduce weight. All internals such as ring frames and bulkheads where required for buckling, slamming, or subdivision are NV A (equivalent to ABS Grade A).

The shell plate thickness of substructures subjected to slamming loads were evaluated in accordance with *DNV-OS-C101* [3]. This approach accounts for the global stresses by a proportional reduction in design bending stress. A correction factor for curved plates was applied to the required thickness for unstiffened shells as permitted by *DNV Rules for Classification of Ships* [5]. An FEA was developed to check ring frames against the slamming loads. A PSF of 1.5 was applied to the pressure and a material PSF of 1.15 was assumed.

Local FEA was performed on the major structural joints as there was no available stress concentration factors (SCF) for the specific arrangements. Loads were applied such that reaction at the fixed end was equivalent to the worst-case free body loads, in order to develop corresponding far field stresses. The calculation of the hot-spot stress at the joint to determine if it required additional reinforcement was performed in accordance with *DNV-RP-C203 Fatigue Design of Offshore Steel Structures* [6]. Local and hot-spot stresses were not to exceed yield as per *DNV CN 34.1 Direct Analysis of Ship Structures* [7]. Hot-spot stresses extrapolated from the FEA were utilized in the fatigue assessment (see 4.3.4).

4.3.2 Bulkheads

Each bulkhead was designed in accordance with the *DNV Ship Rules* [5]. The design pressure was assumed to be the greater of the internal and external pressures (see 4.2.3).

The design of the nacelle end-bulkhead assumed a radially stiffened grillage arrangement to provide access around the generator assembly and accommodate the bolting arrangement. An FEA was

performed adopting the worst-case design condition of the body being entirely submerged. The resulting input loads equaled the highest hydrostatic pressure times a PSF of 1.2 per *DNV-OS-C101* [3] over the entire face; this was conservative but justified as the bulkhead orientation in this case could conceivably vary. Maximum generator torsion was applied with a PSF of 1.35, and a material PSF of 1.15 was assumed.

4.3.3 Mooring, umbilical, and towing attachments

The mooring and towing fittings and respective support structure were designed in accordance with the *DNV-OS-E301 Position Mooring* [8].

The mooring fittings were sized to accommodate the minimum breaking strength of mooring line. Note that the mooring design for WETS was performed by Sound and Sea Technologies on behalf of the US Navy.

The drag of the WEC in its towing configuration was estimated at a nominal towing speed of 3.5 knots, and a load factor of 1.5 was applied to account for wave making drag, and wind and wave loading. Towing was limited to local transportation (e.g., between Honolulu Harbor and WETS) and the analysis considered ultimate loading only. Per *DNV-OS-E301* [8], a towing line was selected with a minimum breaking strength three times the tow load. The towing fittings design was based on the breaking strength of the line.

Hinged load rings were specified for both mooring and towing fittings, to better manage the varying angles. First principle stress and beam analyses were performed to size the pedestals and hull internal backing structure. All structure was assumed to be NV A steel. The umbilical connection design was extended from the aforementioned mooring attachments as the loads were assumed to be comparable.

4.3.4 Fatigue assessment

Fatigue assessment for the prototype WEC structure was carried out in accordance with guidance in *DNV-RP-C203* [6]. Fatigue life for the tubular joint details was calculated as a Miner's sum, assuming a Weibull shape factor of 1.0 and an S-N curve for tubular joints (*DNV-RP-C203* [6]) in seawater with cathodic protection.

Hot-spot stresses were calculated from detailed FEA results for each of the major structural joints (see 4.3.1), reflecting the 50-year return period of the extreme sea state (see 4.2.2), and formed the basis of the fatigue assessment. The maximum stress range conservatively assumed the hot-spot stresses are fully reversing. The average zero-upcrossing period was calculated for the WETS site, assuming a ratio of average zero-upcrossing period to energy period of 0.71. The calculations assumed that the wave zero-upcrossing period was representative of the load and stress response period.

To achieve the required 5-year design life, longitudinal bulkheads in way of the joints were inserted locally with thicker plate. Increasing plate thickness to reduce stress did not improve fatigue life in all cases, because allowable stress reduces as the thickness increases. Improved welds offer an alternate approach to increasing fatigue life, per *DNV-RP-C203* [6]. Full penetration, profiled welds were specified were needed to bring the fatigue life to the required five years.

4.3.5 Fabrication and assembly

The WEC would be constructed of steel. In general, all shell plating will be either rolled or chip broken plate. One exception would be made from pipe. The WEC was modeled in module assemblies to align with the developed build sequence. The build sequence allows for the PTO to be assembled within the nacelle prior to the nacelle being closed up. Estimated weights of assembly modules includes a 3% allowance for welding and millage and a 5% builders' margin.

Lifting points were designed to facilitate assembly and shipping. The lifting pad eyes were designed in accordance with *API RP 2A Planning, Designing and Constructing Fixed Offshore Platforms* [9]. Lifting pad

eyes were designed to the estimated weight of the unballasted WEC. First principles were used to size the pad eyes and an FEA was performed to validate the support structure design.

4.3.6 Support and tiedown

WEC support and tiedown was designed such that the WEC could be transported on a cargo barge from the Pacific NW to Hawaii. The blocking and seafastening arrangement were developed in accordance with *DNV-OS-H202 Sea Transport Operations* [10]. The barge transport design accelerations assumed a nominal 275-foot barge operating in seas with a significant wave height of 6 meters or less. Weather routing was assumed to keep the barge within this operating limit and avoid storms. Three load cases were evaluated representing either the worst-case roll, pitch, or combination of the two from quartering seas. The resulting inertial loads would be resisted by the blocking, seafastenings, and lashings. Overturning moments would be countered by variable blocking pressures. Lateral loads would be absorbed by friction. Lateral loads that exceed the friction force would be reacted by the seafastenings. The predicted accelerations did not tip the overall WEC, but there were localized uplift loads that would be countered by the lashings.

4.3.7 Ballast system

The ballast system functions to control the attitude and stability of the WEC. The permanent ballast tank is subdivided (port to starboard); each subdivision is partially filled with sand, and the remainder flooded with fresh water. Permanent ballast is designed to be filled with the WEC floating horizontally; once filled the permanent ballast tank is sealed. The two variable ballast tanks are designed to be flooded with sea water; as they fill, the ballast tank rotates downward bringing the WEC to its vertical, power production orientation. The ability of the WEC to transition between floating tow and power production configurations via a seawater ballast change, without the need for any external floatation, is a significant step forward from the previous (Baseline) design.

Intact stability was assessed in both the power production and towing orientations. The WEC is subdivided into N watertight compartments and damaged stability analysis validated the design requirement that any one compartment may flood without the WEC sinking or becoming unstable.

Additional details on the ballast system and stability calculations are found in Appendix 11.4

4.3.8 Cost and weight

Cost and weight estimates for the WETS H2 prototype can be found in *WEC Design Documentation* provided as Appendix 11.4.

4.4 Geometric Areas of Interest for Further Optimization

The WETS H2 prototype will be a significant step forward for C-Power's StingRAY WEC technology, and the advantages of the next-generation H2 hull represent significant progress on the Project objectives of increased PWR and decreased LCOE.

In consultation with the designer, Glosten, geometric areas of interest (GAIs) for further optimization were identified. Three criteria were used in assessing potential GAIs (see Figure 1), ensuring that the proposed optimization would be informative, practical, and achievable:

- Potential Impact on Project Objectives
 - Clearly, it is important that any further efforts made within the Project have significant impact on the Project objectives.
- Test Facility Capabilities

- The National Wind Test Center (NWTC), itself a part of the National Renewable Energy Laboratory (NREL), had been contracted to perform structural testing in support of the Project; thus, the capabilities of the NWTC test facility were considered alongside GAIs.
- Schedule and Budget
 - Practically speaking, the remaining Project schedule and budget were also considered in light of the GAIs and associated testing and analysis.



Figure 1 – Criteria for selection of geometric areas of interest for further optimization.

Originally C-Power had identified the float / arm region, and the interface with the nacelle-housed PTO, would be the GAI serving as the focus of optimization. The geometry is complex in this region, and the design relied on relatively thick plate and substantial internal and external stiffening elements to deal with the dynamic loading. A test program aiming to optimize this design would certainly be interesting but would be prohibitively costly, difficult to test at NREL, and ultimately would not yield learning that could be applied elsewhere in the hull structure. A single test specimen fabricated to represent the float / arm / nacelle interface at full-scale would be large and costly. The structural analysis was based on design loads representing five unique stress states that would need to be tested. In any test program, multiple identical tests are required to confirm the soundness of the testing methodology. Each test to failure would yield a single data point.

A decision was made by C-Power and DOE to pursue a mixed materials approach to reducing structural mass and cost. Several subcomponents were identified in which there were structural spans whose simple shapes would be readily fabricated from mandrel wound FRP. It was hypothesized that by substituting FRP for steel where appropriate, significant cost and weight savings would be realized. A specific subcomponent was selected for testing and optimization, with the understanding that the design could be readily extended to other similar subcomponents, magnifying the *potential impact on Project objectives*. To best utilize the remaining *schedule and budget*, a robust test plan consisting of coupon and full-scale sectioned joint testing was conceived. The draft test plan was developed in consultation with NREL, ensuring that the work was within the *test facility capabilities*. In this manner the GAI selection criteria were satisfied.

The mixed materials concept and the laboratory test plan are discussed in greater detail in Section 5. A summary of the prototype H2 WEC hull and mixed materials concept designs are provided in Appendix 11.6.

5 TEST-SUPPORTED MIXED MATERIALS OPTIMIZATION

5.1 Mixed Materials Concept

A large structural subcomponent of the H2 WEC was selected for analysis, testing, and optimization. There were two identical instances of this subcomponent, and each was a large cylinder (approximately 13 m long by 4 m diameter) rigidly connected at both ends via complex joints. The concept mixed materials design replaced an 8 m, unsupported span of steel with a composite laminate.

The concept design of the hybrid structural subcomponent (i.e., the test article) is described in detail in *Test Article Design Technical Memo* (Appendix 11.7).

The design laminate was a simple cylinder with a monolithic layup schedule, based on processes from Ershigs, a long-time FRP fabrication partner of C-Power. The Ershigs process for constructing large filament-wound (FW) tanks is to use a spray chop gun to add chopped strand mat (CSM) as the first layer against the mandrel, and then consolidate over that CSM with a full layer of filament-wound e-glass. Consecutive double layers of filament windings were added interspersed with a hand laid stitched fiberglass unidirectional fabric (U, or UNI) supplied by Vectorply. FW angles were specified at $\pm 65^\circ$ from the mandrel axis, and a single layer comprises windings in both directions. The unidirectional fabric was oriented with the fibers parallel to the mandrel axis. Note that the CSM does not contribute structurally to the laminate, and the fabricator may use it to maintain laminate quality as necessary. An epoxy vinyl-ester resin was specified. A stitched fiberglass quadraxial fabric (QUAD) was recommended by Ershigs should fabricated internal stiffening details add sufficient value to justify their cost.

The concept joint design was an adhesively bonded double lap consisting of two steel rings capturing the edge of the composite shell (Figure 2). The connection joints between the composite cylinder and the adjacent steel structure were designed to be fault tolerant and simple to assemble. A 45° angle was specified at the terminus to minimize cleave and peel forces.

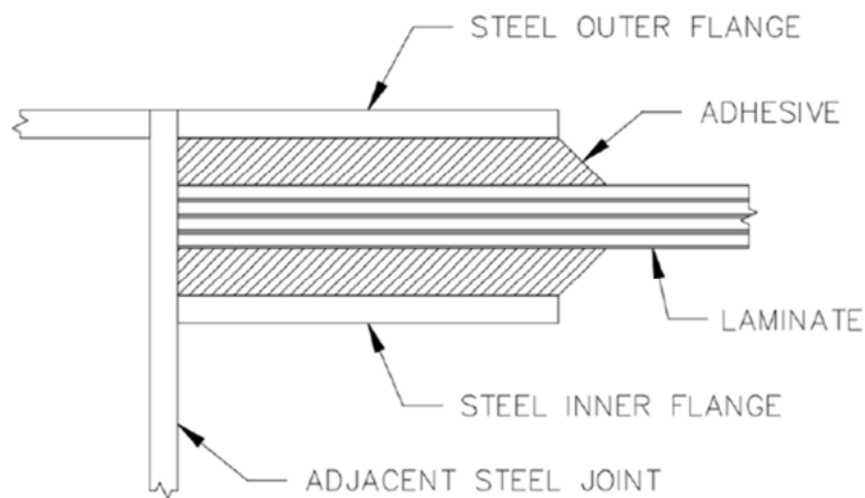


Figure 2 – Double lap shear joint concept detail.

The concept laminate was developed by Glostén, guided by *DNVGL-ST-C501 Composite Components* [11]. The Tsai-Wu failure criterion (TWFC) was used for evaluation of composite strength, and a FEA model comprising the FRP cylinder was developed. Siemens Femap 11.4.2 with NX Nastran was used to mesh, analyze, and post-process the geometry. The materials modelled were developed from manufacturers'

specification sheets, with some corrections applied following *DNVGL-ST-C501* [11]. The boundary conditions modeled the steel structure with its flange connection. The load cases were derived from the *WEC Design Documentation* (Appendix 11.4). The FEA results were used to specify a concept layup schedule, and a required adhesive strength.

The limiting load case for both the laminate and the adhesive joint was the slamming load case. The concept layup schedule was 26mm thick solid laminate [3.0oz CSM, 1FW, 9(1UNI,2FW), 1.5oz CSM]. The bondline loading was dominated by shear. The *double* lap shear (DLS) joint was recommended over a *single* lap to halve the required adhesive strength. The double lap shear detail was preferred over an extension of the steel flange because it added additional robustness. It was found that as the flange gets longer, the inboard edge attracts more load which strains the bondline load distribution assumptions. Additionally, since the double lap joint would utilize adhesive on both sides of the laminate, the adhesive bondline thickness would be better controlled for geometric deviations between the steel flanges and the FRP circumference.

A weight savings of ~50% over the baseline steel design was estimated at this stage.

5.2 Laboratory Testing

5.2.1 Test program and objectives

The laboratory test program, which is described in detail in *Composite Test Program Memo* (see Appendix 11.8), had two primary objectives:

- To obtain precise design values for the materials and processes to be used for the laminate fabrication, and
- To test the suitability of multiple candidate adhesives, validating the feasibility of the DLS joint for this application.

Coupon testing was necessary for the composite structure to obtain precise design values for the fabricator's materials and processes. Standard practice in the marine industry is to collect design data this way for each material and process used in manufacture. Statistical methodology detailed in *DNVGL-ST-C501* [11] defines a partial material factor based on the number of coupon tests completed for each material property. A higher number of data points allows higher confidence in the measured properties, resulting in lower design factors and a more efficient structure. Coupon tests were performed utilizing a universal test machine (UTM) under the direction of an experienced test engineer.

The composite laminates were generalized as orthotropic two-dimensional materials modeled as plates in FEA. This assumption was made because the out-of-plane properties were much smaller than the in-plane properties. The specific material properties required for this type of analysis are:

- Elastic modulus in the fiber (1) and cross-fiber (2) directions (E_1, E_2)
- Shear modulus in the 1-2 plane (G_{12})
- Poisson's ratio in the 1-2 plane (ν_{12})
- Tensile strength in the 1 and 2 directions (σ_{1t}, σ_{2t})
- Compressive strength in the 1 and 2 directions (σ_{1c}, σ_{2c})
- Shear strength in the 1-2 plane (τ_{12})
- Laminate layer thickness (t_i)
- Laminate layer fiber volume fraction (FVF)

A test matrix using American Society for Testing Materials (ASTM) standards was developed to obtain the data necessary for calculation of the requisite material properties using FW, UNI, and QUAD coupons.

The global design loads are carried by shear within the steel-to-composite DLS joints. These can be modelled in the UTM using full-scale section joints, fabricated using coupons of full-scale laminate thickness adhesively bonded to steel coupons. These tests were used to assess the suitability of multiple adhesives at multiple thicknesses, with the goal of finding the least-cost, highest performing adhesive configuration.

Three different candidate adhesives (Plexus MA560-1, Araldite 2013, and Araldite 2015) were selected based on:

- strength in conjunction with structural adherends (steel and vinyl-ester resin FRP),
- working time,
- gap-filling,
- low-temperature post-cure (room temperature preferred)
- marine applicability,
- shock tolerance (i.e. low modulus).

Plexus MA560-1 is a two-part methacrylate adhesive, while Araldite 2013 and 2015 are both two-part epoxy-paste adhesives.

The large diameter structural components necessarily deviated from ideal geometry (e.g., diameter, concentricity, eccentricity, etc.), especially the FRP. To accommodate practical fabrication and manufacturing, and allow for a more fault tolerant assembly, significant gap-filling capability is preferred (allowing for greater bondline thickness). Thus, the intent was to test over a range of thicknesses and identify adhesives with sufficient strength at significant thicknesses. Plexus MA560-1 adhesive was tested at thickness of 6.4, 12.7, and 19.0 mm (0.25, 0.50, and 0.75 in.); the two Araldite adhesives were tested at 6.4 and 12.7 mm bondline thickness, on the recommendation of the manufacturer.

The DLS test plan specified a modified ASTM lap shear test to assess ultimate strength of the adhesive joint. The modification was necessitated by the adhesive thicknesses, which deviate from the ASTM standard. The test plan called for two adhesive configurations (defined by an adhesive and a thickness) down selected based on comparative ultimate strength results, with consideration of bondline thickness. The goal was to balance joint strength and manufacturability.

Following the ultimate strength lap shear tests, fatigue tests were run on the two down-selected adhesive configurations. Final assessment of adhesive suitability for the DLS design could then be made.

In total, the test program specified 163 coupon tests and 85 DLS tests.

5.2.2 Test specimens

Three different composite material panels were fabricated for coupon testing, along with concept laminate panels for full-scale sectioned DLS testing. Coupon panel and coupon definitions are given in *WEC Design Alternative Composites Test Program Panels* (see Appendix 11.9).

The concept laminate and FW panels were formed on a mandrel. The UNI and QUAD panels were hand laid and vacuum infused, respectively, on a table. The concept laminate, FW, and UNI panels were fabricated by Corrosion Companies Inc. (CCI), while the QUAD panels were fabricated by Ershigs.

Note that C-Power had originally planned for Ershigs to design the concept laminate and fabricate all panels. However, other commitments precluded Ershigs full involvement; Glosten was then engaged to design the concept laminate, and CCI to fabricate most of the panels.

CCI wound the FW and concept laminate panels at a diameter of 3.66 m (12.0 ft). The large diameter winding was necessary simulate the fabrication conditions of the WEC components, and to minimize out-

of-plane deviation of the coupons. The 12 ft diameter surface was built up over a 6 ft mandrel to facilitate concurrent fabrication projects at CCI. See Figure 3 for pictures of the 12 ft diameter mold, and the helical filament winding process. To further simulate the fabrication conditions of the WEC components, CCI waited in between winding layers before initiating the next layer; this allowed for a degree of curing between layers corresponding to expectations for a the larger WEC component.



Figure 3 – Filament winding mold, and helical winding process.

Panels were shipped to NREL where they were inspected. All coupons were cut to shape and prepared for testing by NREL.

The DLS test specimens were manufactured by NREL from concept laminate coupons, steel coupons, and adhesive. Composite coupons were waterjet cut to size by Colorado Waterjet. Steel coupons were waterjet rough-cut to size by Colorado Waterjet from 12.7 mm thick AH-36 steel plate and were then machined to size and 11.1 mm thickness at NREL. The steel coupons were intended to be 25.4 mm wide, but the waterjet cutting produced a slight taper, and the coupons were machined down to 24.1 mm to ensure a smooth surface and rectangular cross section. Steel and composite coupons, machined ready for DLS assembly, are shown in Figure 4.

NREL designed and constructed five 'identical' assembly fixtures for DLS specimen fabrication. The test fixture was designed to maintain a 152 mm (6 in.) bondline length at the interface of the composite coupon and adhesive given the three bondline thicknesses of 6.4, 12.7, and 19.0 mm. A 45° taper was maintained at each end of the bondline and thus the bondline length at the steel interface was 165 to 190 mm long. An assembled DLS specimen curing in an assembly fixture, and a collection of cured and ready-to-test DLS specimen, are shown in Figure 5.

Due to the limitations of the UTM grips and the thickness of the concept laminate, it was necessary to design the DLS specimens such that the thinner steel coupon would be held by the UTM grips. The relative positions (inner and outer) of the steel and FRP were swapped for the DLS specimens. The difference, which can be seen by comparing the schematic of the joint concept in Figure 2 with the photograph of the

test specimen in Figure 5, was not expected to influence the test results as shear load is still carried by the adhesive and the bonds with the steel and composite adherends.

Coupon and DLS specimen fabrication are described in detail in *C-Power Coupon and Double Lap Shear Specimen Test Report* (see Appendix 11.10).



Figure 4 – Steel and composite coupons prior to assembly into DLS specimens.

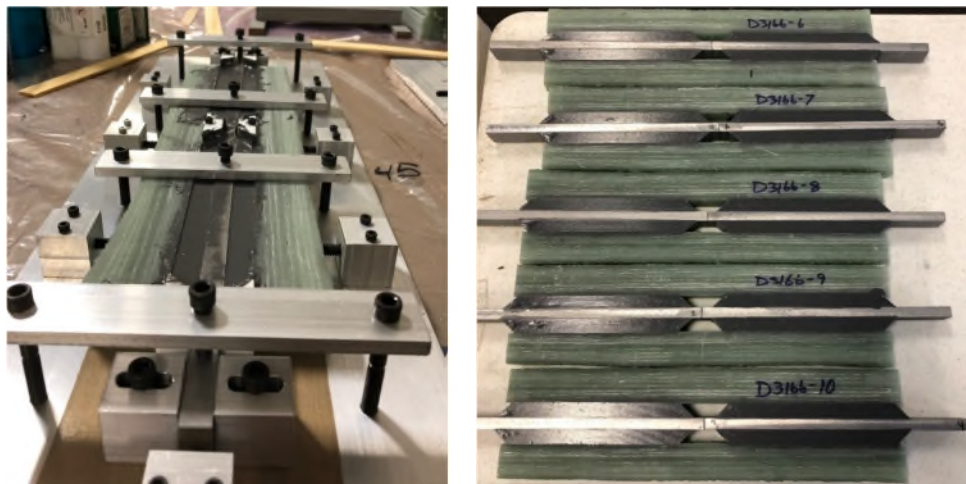


Figure 5 – DLS specimen curing in fixture (left), and five cured DLS specimens (right).

5.2.3 *Fiber-reinforced plastic coupon and full-scale sectioned adhesive joint testing*

Test set up and results are described in detail in *C-Power Coupon and Double Lap Shear Specimen Test Report* (see Appendix 11.10). Unlike the other appendices attached to the *Final Technical Report*, the *Test Report* is non-confidential. All laboratory testing was performed at NREL's NWTC in Boulder, CO.

The following ASTM standards were followed in coupon testing:

- *D3039 Tensile Properties of Polymer Matrix Composite Materials*
- *D6641 Compressive Properties of Polymer Matrix Composite Materials Using a Combined Loading Compression (CLC) Test Fixture*
- *D7078 Shear Properties of Composite Materials by V-Notched Rail Shear Method*

- *D7291 Through-Thickness “Flatwise” Tensile Strength and Elastic Modulus of a Fiber-Reinforced Polymer Matrix Composite Material*
- *D3171 Constituent Content of Composite Materials*

Coupon testing was performed on filament wound FW, uniaxial (UNI), and QUAD coupons in order to determine their relevant material properties. The derived characteristic material properties of FW and UNI materials are listed in Table 2 and Table 3 (see 5.3.1), along with indication of which ASTM tests results were used in the calculations. A total of eight coupon tests for each material / orientation combination were specified; however, some test results were rejected (see the *Test Report* for details) and Table 2 and Table 3 indicate the number of valid test results used for calculations.

Mass properties and FVF were determined from tests of nine specimens (three each for FW, UNI, and QUAD) following *D3171*.

The *D7291* test (“flatwise” through-thickness) had been specified for tensile strength perpendicular to the fiber orientation, however it is more appropriate for interlaminar tensile strength which is not needed under the two-dimensional material model assumed. A decision was made instead test additional coupons following *D3039*, cut such that loading would be perpendicular to the fibers (direction 2). This was done with extra UNI material, and the results were used for FW as well; because this is a matrix property, the assumption was made that tensile strength in direction 2 should be similar for both materials.

Static testing of DLS specimens was conducted following *ASTM D5856 Lap Shear Adhesion for Fiber Reinforced Plastic (FRP) Bonding*. A total of 37 specimens were tested, with seven adhesive / bondline thickness configurations. Following static testing a down-selection was made to 0.5 in. MA560-1 and 0.5 Loading.

Application of the test results to C-Power design and optimization are covered in Section 5.3.

5.3 Mixed Materials Optimization

This Section summarizes the derivation of constituent material characteristic properties; optimization of the concept laminate; assessment of tested adhesive configurations and DLS joint feasibility; and assesses the potential impact of the mixed materials concept on the prototype H2 WEC. This analysis is covered in detail in *Optimization Memo*, which is provided in Appendix 11.11.

5.3.1 Laminate material properties and optimization

The structural analysis described in this Section is based upon characteristic values of material properties derived from the laboratory test results, following guidance from *DNVGL-ST-C501* [11].

Relevant test results, along with the characteristic values, are detailed in Table 1 and Table 2 below; recall from Section 5.2.1 that direction 1 is the fiber direction and direction 2 is in-plane and orthogonal. The ASTM test results used to calculate the characteristic value are listed; as the *Test Report* (see Appendix 11.10) is organized by ASTM test, it is easy to find the relevant content. The QUAD coupon results are not covered in this document, as they were not utilized in the concept design or optimization.

For elastic properties, the characteristic values are simply the mean value of valid test results. For strength properties, the characteristic value is reduced from the mean by a specified number (k_m) of standard deviations. Note that FW tensile strength perpendicular to the fibers (direction 2) was not tested but assumed to be similar to UNI as this is a matrix dominated property and the same resin was used for both.

In addition to the elastic and strength material properties, the measured thickness and density of the constituent materials are relevant to the laminate design and optimization. Measured thickness, density, and FVF are listed in Table 4.

Table 2 – Material properties determined from filament wound (FW) coupons.

Property	Units	Mean	std	pstd	N tests	k _m	Char. Value	Test Report source
Elastic modulus, dir. 1 (E_1)	Gpa	26.0	1.38	0.05	5	-	26.0	D3039, Table 2-5
Elastic modulus, dir. 2 (E_2)	Gpa	16.8	2.34	0.14	5	-	16.8	D6641, Table 3-3
hear modulus, 1-2 plane (G_{12})	Gpa	5.93	0.59	0.10	8	-	5.93	D7078, Table 4-6
Poisson's ratio, 1-2 plane (ν_{12})	-	0.503	0.055	0.11	4	-	0.503	D3039, Table 2-5
Tensile strength, dir. 1 ($\hat{\sigma}_{1t}$)	Mpa	503	22.7	0.05	5	2.3	451	D3039, Table 2-3
Compressive strength, dir. 1 ($\hat{\sigma}_{1c}$)	Mpa	371	50.2	0.14	8	2.6	241	D6641, Table 3-3
Tensile strength, dir. 2 ($\hat{\sigma}_{2t}$)	Mpa	20.6	2.03	0.10	6	2.8	14.9	UNI result, see below
Compressive strength, dir. 2 ($\hat{\sigma}_{2c}$)	Mpa	113	17.7	0.16	8	2.6	66.6	D6641, Table 3-3
Shear strength, 1-2 plane ($\hat{\sigma}_{12}$)	Mpa	108	11.4	0.11	8	2.6	78.0	D7078, Table 4-6

Table 3 – Material properties determined from uniaxial (UNI) coupons.

Property	Units	Mean	std	pstd	N tests	k _m	Char. Value	Test Report source
Elastic modulus, dir. 1 (E_1)	Gpa	32.8	4.69	0.14	8	-	32.8	D3039, Table 2-5
Elastic modulus, dir. 2 (E_2)	Gpa	8.20	1.03	0.13	4	-	8.20	D6641, Table 3-3
Shear modulus, 1-2 plane (G_{12})	Gpa	2.00	0.05	0.03	8	-	2.00	D7078, Table 4-7
Poisson's ratio, 1-2 plane (ν_{12})	-	0.418	0.020	0.05	8	-	0.418	D3039, Table 2-5
Tensile strength, dir. 1 ($\hat{\sigma}_{1t}$)	Mpa	573	26.2	0.05	8	2.2	515	D3039, Table 2-3
Compressive strength, dir. 1 ($\hat{\sigma}_{1c}$)	Mpa	306	25.7	0.08	7	2.8	234	D6641, Table 3-3
Tensile strength, dir. 2 ($\hat{\sigma}_{2t}$)	Mpa	20.6	2.03	0.10	6	2.8	14.9	D3039, Table 2-11
Compressive strength, dir. 2 ($\hat{\sigma}_{2c}$)	Mpa	75.9	3.36	0.04	8	2.6	67.2	D6641, Table 3-3
Shear strength, 1-2 plane ($\hat{\sigma}_{12}$)	Mpa	35.8	1.57	0.04	8	2.6	31.7	D7078, Table 4-7

Table 4 – Thickness, density, and FVF for FW and UNI materials.

	Thickness [mm]	Density [kg/m ³]	FVF
FW	1.44	1880	0.509
UNI	0.797	1540	0.291

Like the concept design analysis summarized in Section 5.1, an FEA model comprising the FRP subcomponent was developed and assessed against design loads. ANSYS Mechanical v16 was used to mesh, analyze, and post-process the results. This analysis was performed by C-Power differs from the concept design analysis performed by Glostin in several ways. The two most significant differences, aside from the use of characteristic values derived from test results, are briefly highlighted here:

- The load and resistance PSF's in the optimization analysis follow more closely to those utilized in the prototype H2 WEC hull design, and are significantly larger than those used for the mixed materials concept design, and
- The load cases in the optimization analysis follow more closely to those utilized in the prototype H2 hull design; the load cases used for mixed materials concept design grossly exaggerated structural loading.

Various laminate layups were modeled and post-processed for TWFC, to determine the fewest layers necessary to keep the maximum TWFC below unity. The resulting optimized laminate [1FW,7(1UNI,2FW),1UNI,1FW] utilized fewer layers overall than the concept design [1FW,9(1UNI,2FW)]. The thickness of the optimized laminate was calculated as 29.4 mm, using the constituent ply thicknesses measured in testing.

The maximum TWFC for the optimized laminate was calculated as 0.88 in the most limiting load case (slamming). The TWFC distribution for the slamming load case, for the outermost layer (where the maximum TWFC occurs), is depicted in Figure 6. Note that the maximum TWFC occurs in the outermost UNI layer for most load cases but occurs in the outermost FW layer for the slamming case.

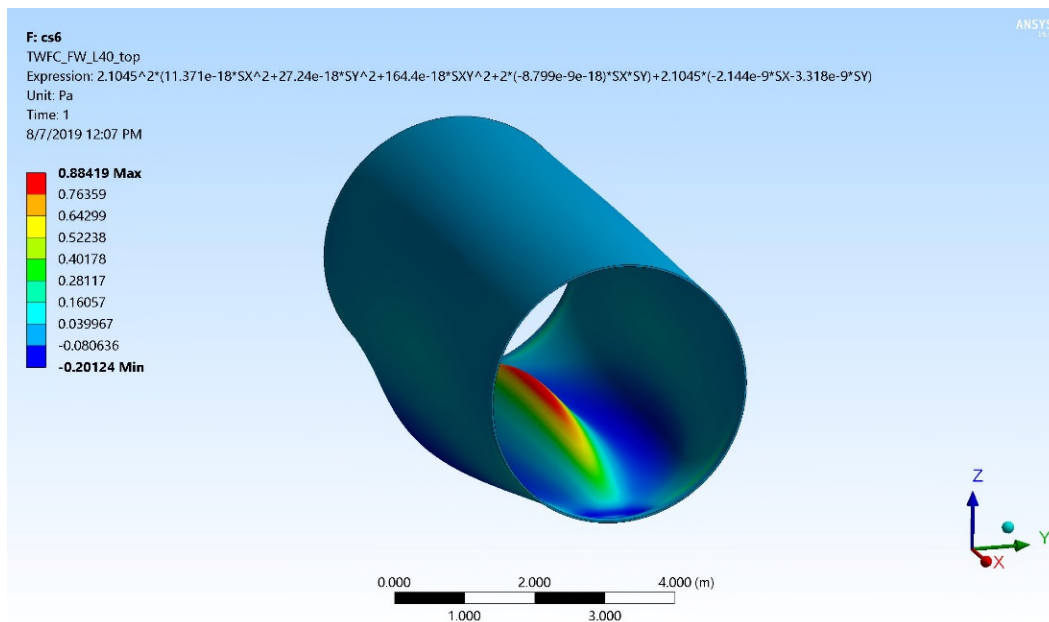


Figure 6 – Tsai Wu Failure Criteria for slamming load case.

Design loads for the adhesive bond were derived from the FEA. Nodal loads at the fixed boundaries were applied to a discretized area representative of the double lap shear joint (DLS), resulting in a bondline stress distribution about the circumference of the bonded joints. DLS test results and design feasibility will be discussed in the following Section.

5.3.2 Adhesive joint feasibility

5.3.2.1 Ultimate limit

The expected stress distribution circumferentially around the adhesive joint was estimated from FEA, as discussed in the previous Section, with the slamming load case driving the design and yielding a characteristic ultimate stress of 2.35 MPa. Note this value was a mean stress calculated over a discretized bond area of 25 (circumferential, element size) by 150 mm (axial, steel flange depth).

Adhesive bond theory (specifically, the improved shear-lag based solution for double lap shear joints [12]) was used to estimate the axial stress distribution. The maximum shear stress, relative to the mean stress, was expected to rise with increasing adhesive stiffness. For a thickness of 12.7 mm (0.50 in.), the ratio of maximum to mean shear stress was calculated as 1.2, 1.6, and 2.1 for Plexus MA560, Araldite 2015, and Araldite 2013 respectively. For a thickness of 6.4 mm (0.25 in.) the maximum stresses increased by about 20%, and for a thickness of 19.0 mm (0.75 in.) the maximum stresses decreased by about 10%. Strain gauges were installed along select DLS bondlines and the data recorded supported the theoretical analysis; these data are presented in the *Test Report* (see Appendix 11.10). However, it was difficult to draw detailed conclusions as the strain was measured at only three locations along select bondlines, and the area covered by a shear strain gauge (5.72 by 8.13 mm) was substantial in comparison to the bondline dimensions. In the present analysis, assessment of DLS strength was based on mean stress over the bonded area.

Testing was conducted following guidance from ASTM D5868, and test specimens loaded to failure. Typically, the steel-to-adhesive bond was observed to be the primary failure; cohesive failure of the adhesive or laminate failure was also observed but theorized to result from peel and cleave forces introduced following the primary failure. Typically, Plexus failures at the steel-to-adhesive bondline were rough with adhesive still attached to the steel. Araldite failures at the steel-to-adhesive bondline were very smooth with minimal adhesive remaining on the steel. Descriptions of DLS specimen failures are detailed in the *Test Report* (see Appendix 11.10). A typical failure is depicted below in Figure 7.

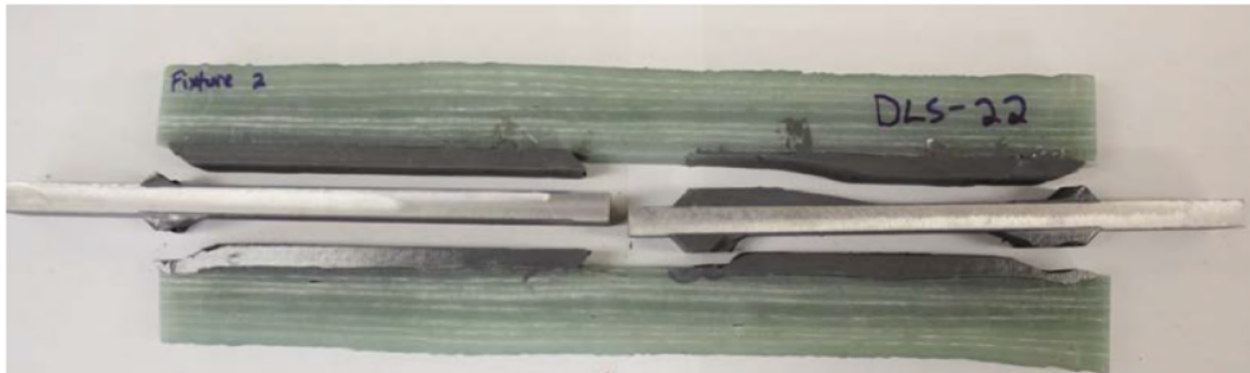


Figure 7 – Typical double lap shear static testing failure.

Mean and characteristic values of shear strength were calculated for all adhesive configurations tested (Table 5). The characteristic values were calculated as the mean of valid test results, minus a specified number (k_m) of standard deviations. Values of k_m were taken from *DNVGL-ST-C501* [11].

The relatively small number of valid test results, along with the level of variance in results, resulted in inconsistent reductions in characteristic strength. While use of the characteristic values was important in design for risk mitigation, the mean shear strength may give a more accurate representation of the relative performance of the adhesive configurations. Considering the mean shear strength values, one sees that the shear strength tends to reduce with increased bondline thickness (0.25 in. Plexus contradicts this trend for reasons that are unclear).

All adhesive configurations tested exhibited sufficient strength to satisfy the characteristic ultimate stress of 2.35 MPa; using the characteristic design values, utilization ranges from 0.40 to 0.70.

Due to the long test times required for fatigue testing, it was necessary to down select to two adhesive configurations. Mean shear strength values were used as the basis for down select, for reasons discussed above. Plexus MA560 and Araldite 2013 both exhibited high strength (11.8 and 11.7 MPa mean strength,

respectively) at a relatively thick bondline (12.7 mm, or 0.50 in.) The only adhesive configuration with a higher mean strength was the 6.4 mm (0.25 in.) Araldite 2013; however, the higher tolerance requirements associated with the thinner bondline do not justify the moderate strength increase. Fatigue testing Araldite 2013 at both thicknesses was considered; while having comparative fatigue data at two bondline thicknesses would be informative, it was decided that having fatigue data for two different adhesive types provided greater value. Therefore 12.7mm (0.50 in.) Plexus MA560 and 12.7mm (0.50 in.) Araldite 2013 were down selected for fatigue testing.

Table 5 – Characteristic shear strength of double lap shear joints.

Adhesive configuration	Units	Mean	std	pstd	N tests	k_m	Char. value	Utilization
Plexus 0.25 in.	MPa	10.9	0.34	0.031	4	3.2	9.79	0.48
Plexus 0.50 in.	MPa	11.8	0.35	0.030	5	2.9	10.8	0.44
Plexus 0.75 in.	MPa	11.5	0.86	0.075	5	2.9	8.98	0.53
Araldite 2013 0.25 in.	MPa	12.7	0.31	0.025	5	2.9	11.8	0.40
Araldite 2013 0.50 in.	MPa	11.7	1.55	0.132	4	3.2	6.76	0.70
Araldite 2015 0.25 in.	MPa	10.9	0.19	0.018	2	3.7	10.2	0.46
Araldite 2015 0.50 in.	MPa	10.8	0.44	0.041	2	3.7	9.16	0.52

5.3.2.2 Fatigue Limit

Two adhesive configurations were selected for fatigue testing; Plexus MA560-1 and Araldite 2013, both at 12.7 mm (0.50 in.) bondline thickness. Testing was conducted following guidance from ASTM D3166 and is detailed in *Test Report* (see Appendix 11.10). Fatigue analysis was based upon the fatigue test results (S-N data) and followed guidance from *DNVGL-RP-C203* [6], and *DNVGL-ST-C501* [11].

The results from all fatigue tests that cycled to failure are depicted below in Figure 8; there are 24 Plexus MA560 results, and 23 Araldite 2013. Results are plotted on log-log scales, as cycles-to-failure versus the stress range at which they were cycled. Considering the fatigue test results, along with the ultimate stress obtained from static testing, a two-slope S-N curve was assumed.

A subset of stress ranges (mid- to high-cycle region) was selected for fitting the primary S-N curve; these data are indicated by blue circles in Figure 8. A least-squares fit was performed on these data, providing a mean S-N curve for the mid- to high-cycle region. Note that one Araldite result was rejected as an outlier (plotted as a yellow 'x'). A least-squares fit was performed on the remaining low-cycle data, with the result constrained to pass through the mean ultimate stress from static testing.

Similar to the characteristic design values discussed in Section 5.3.1, design S-N curves were also assessed. Following guidance provided in *DNVGL-RP-C203* [6], the mean S-N curve was shifted by a specified number (c) of standard deviations of test data $\log_{10} N$. The standard deviation of the primary S-N curve data was used (mid- to high-cycle).

Fatigue life was calculated as a Miner's sum, assuming a Weibull shape factor of 1.0. A mean zero-upcrossing period of 6.68 s was calculated for the prototype deployment site, assuming a Pierson-Moskowitz spectral shape and a ratio of mean zero-upcrossing period (T_z) to energy period (T_e) of 0.827. The fatigue life calculations assumed that the stress response period was characterized by the zero-upcrossing period.

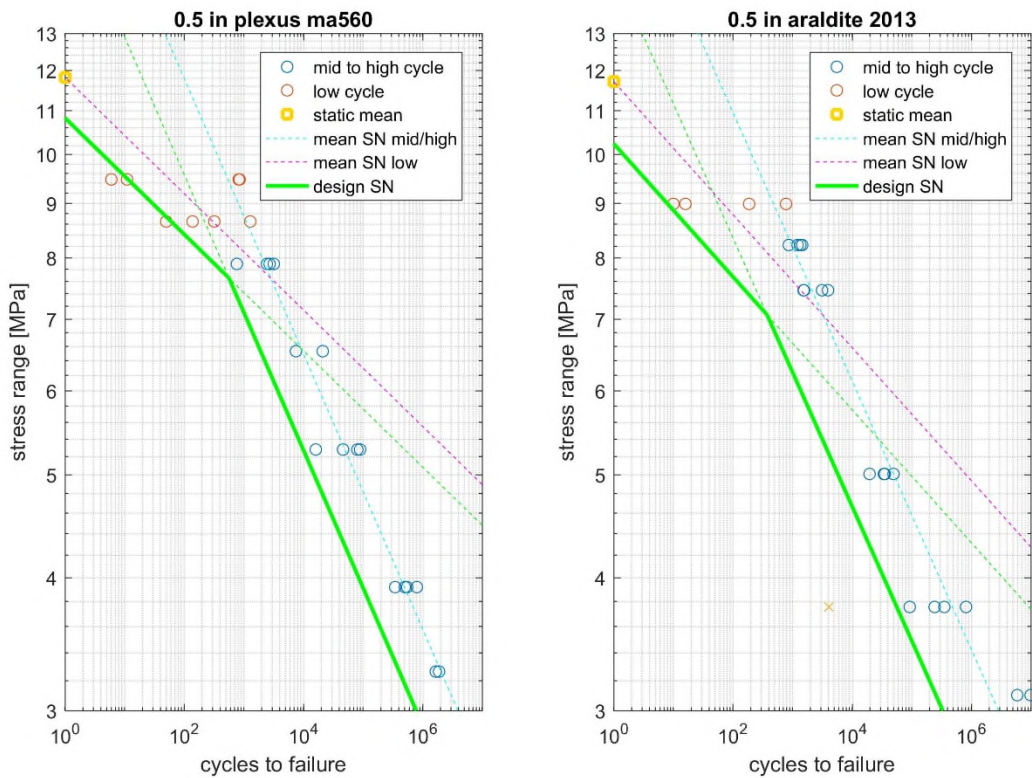


Figure 8 – Fatigue data and SN curves for 0.5 in. Plexus MA560 and Araldite 2013.

Based on the design S-N curves derived from DLS fatigue testing, the fatigue life of the adhesive joint under the most conservative assumption of fully reversing maximum stress was 1930 and 890 years for Plexus MA560 and Araldite 2013, respectively.

Considering that the prototype WEC has a design life of 5 years, and that the eventual commercial WEC will have a design requirement of a 20-year life, this fatigue analysis supports the feasibility of the DLS adhesive joint design using either adhesive configuration tested.

5.3.3 Hybrid Structure Impact

The impact of a hybrid FRP/steel structure on the prototype H2 WEC was estimated in terms of cost and weight. Estimated costs were for fabrication only, and did not include engineering, coatings, delivery, installation, etc. Estimated mass assumed a density of 7800 kg/m^3 for steel; using measured ply density and thickness values from Table 4, the density for the optimized laminate was calculated as 1810 kg/m^3 .

Cost and weight estimates were for those sections of the hull components that were being considered for replacement with FRP. Steel cost estimates assumed a labor rate of 75 \$/hour, a fabrication rate of 150 hours/long ton, and a material cost of 0.754 \$/lb. The estimated fabrication cost for the FRP alternative was based on a quote from Ershigs [13] for concept design of the hybrid structural subcomponent (i.e., test article), and supplier quotes for the two candidate adhesives [14], [15].

There were several hull components of the prototype WEC with significant structural similarities to the test article. Although not investigated explicitly within this 6610 Project, it is reasonable to assume that a similar hybrid construction could readily be adapted for these components as well. Rather than developing layup schedules for each of these sections, an assumption was made that required FRP

thickness is proportional to the required steel thickness determined in prototype design. The estimated cost of the steel and FRP sections were assumed to be proportional to their mass.

Assuming the mixed materials concept is applied only to the two test article components, there was an estimated savings of 6.74 tonnes and \$93.3k per WEC. Assuming the mixed materials concept was applied to all of the structurally similar components (see Appendix 11.11) there is an estimated savings of 13.0 tonnes and \$181k per WEC.

Note that this analysis was for the prototype H2 WEC; the impact on 6610 Project metrics will be covered in the following Section.

6 PROJECT IMPROVEMENTS AND IMPACT

6.1 Next-Generation WEC Hull

The StingRAY WEC architecture has undergone a generational advancement. The H1 WEC architecture, developed under 5930, was examined for cost reduction opportunities in conjunction. The resulting H2 WEC offers numerous benefits. In alignment with the 6610 Project objectives and a desire to capitalize on these technical advancements, DOE and C-Power agreed that the improved H2 WEC architecture should be integrated with the 6610 Project. Under 6610, the H2 WEC was progressed from concept to final design with structural drawings.

The H2 WEC concept centers about an architecture that allows for a more efficient use of structural and power generation components, along with simplified component geometries aimed at reducing manufacturing costs; these changes result in lower cost and weight. The new H2 WEC architecture also exhibits a significant improvement in power performance. The H2 WEC can transition between floating tow and power production configurations via a seawater ballast change, without the need for at-sea installation of external buoyancy components which were required by the H1 WEC, reducing operations complexity and cost.

The H2 WEC hull design is described in detail in the following documents provided as appendices:

- *CPower WEC Design Documentation* (see Appendix 11.4).
- *CPower WEC Structural Arrangement* (see Appendix 11.5).

6.2 Test-Supported Mixed Materials Optimization

A mixed materials concept to further optimize the H2 WEC was developed and verified via testing and analysis. This approach substituted FRP for steel where appropriate (i.e., structural spans whose simple shapes are readily fabricated with mandrel-wound FRP), resulting in additional cost and weight savings.

A robust testing program yielded characteristic values for the laminate constituent materials, allowing for Project laminate optimization as well as additional component design as potential future work. The test program also yielded ultimate and fatigue characteristics for three candidate adhesives over a range of practical bondline thicknesses.

The testing and analysis led to a laminate that was optimized for the 6610 Project test article, and that can be readily scaled and applied to several similar subcomponents. Additionally, the feasibility of the DLS adhesive joint design fundamental to the mixed materials concept was validated.

The mixed materials concept, testing, and optimization are described in detail in the following documents provided as appendices:

- *Test Article Design Technical Memo* (see Appendix 11.7).

- *C-Power Coupon and Double Lap Shear Specimen Test Report* (see Appendix 11.10).
- *Optimization Memo* (see Appendix 11.11).

6.3 SPA and LCOE Impact

The SPA metrics identified in the Statement of Project Objectives (SOPO) are the PWR based on system AW and DW consideration where:

$$PWR = \frac{\text{Rated Capacity (kW)} \times \text{Capacity Factor}}{\text{Weight (metric tons)}}$$

The goal of the 6610 Project was to allow for AW PWR to increase by 64% and DW PWR to increase by 15% (see Table 6), meeting Marine and Hydrokinetic SPA Funding Opportunity Announcement Goal 1. In addition to the improvement in SPA metrics, Project impact was demonstrated via a decrease in LCOE from Baseline H1 to Final H2 WEC.

Annual energy production (AEP) and LCOE calculations and models were compliant with Department of Energy (DOE) guidance [16]. The impact of Project improvements on SPA metrics and LCOE as well as models, assumptions, and calculations are covered in detail in *Impact Assessment* (see Appendix 11.12). The hydrodynamic modeling and subsequent analyses used to assess AEP are described in *Energy Production Assessment for DOE LCOE and SPA Reporting* (see Appendix 11.13). Power and losses as a function of sea states, along with energy production in the reference resource, are presented in *Baseline and Final TAEP Calculations* (see Appendix 11.14).

Table 6 – Targeted system improvements goals.

	Improvement Goal	
Baseline -> Final	AW PWR	DW PWR
S1 -> S2	64%	15%

The Baseline (S1) conformed to the StingRAY H1 WEC architecture, where StingRAY indicates C-Power’s MCBH WETS scale WEC technology and H1 WEC indicates C-Power’s three-body hull design that was current at 6610 proposal submission.

The Final WEC (S2) conformed to the StingRAY H2 WEC architecture, where H2 indicates C-Power’s hull, whose detailed design was accomplished within this 6610 Project. The prototype H2 WEC was designed specifically for testing in the WETS resource and was undersized with respect to the reference resource and the H1 WEC Baseline. To facilitate an accurate comparison, the WETS H2 WEC design was scaled up such that S1 and S2 total active mass were comparable. The mixed materials design was applied to the subcomponents discussed in the *Optimization Memo* (see Appendix 11.11).

The Project SPA metric improvement goals were substantially surpassed, with improvements of 99.4 and 88.0% for AW and DW PWR, respectively. Although there was no specific goal established for LCOE improvement, the 54.1% reduction represents a Project success.

Table 7 – Targeted and actual SPA metric and LCOE improvements.

Metric	Goal	Actual
Active weight (AW) PWR	64.0%	99.4%
Dry weight (DW) PWR	15.0%	88.0%
Levelized Cost of Energy (LCOE)	n/a	-54.1%

7 CHALLENGES AND LESSONS LEARNED

The H1 WEC architecture developed under 5930, was examined for cost reduction opportunities. The resulting H2 WEC offered numerous benefits including lower part count, more efficient use of materials, lower-cost ballast, and increased power performance. The H2 WEC size was optimized specifically the WETS deployment location, resulting in a WEC size somewhat smaller than the H1 WEC, yielding decreased CAPEX for the prototype deployment. In alignment with the 6610 Project objectives and a desire to capitalize on these technical advancements, DOE and C-Power agreed that the improved H2 WEC architecture should be integrated with the 6610 Project.

After spending some time on preliminary H2 WEC structural design, Ershigs (an FRP design and fabrication partner) withdrew as the structural designer for H2. A search for a new designer with naval architecture experience was undertaken, and Glosten was contracted to take on the role. With the change from Ershigs to Glosten, the requirement for FRP hull fabrication was relaxed in favor of steel. Use of steel brought the benefits of lower cost for a one-off prototype, risk reduction (more industry experience and lower safety factors), better tolerances in a one-off prototype, and adaptability in fabrication and system integration.

The fatigue assessment performed indicated that some joint details did not meet the requisite design life, and that increasing plate thickness did not improve design life in all cases. The conservative nature of a key assumption in the fatigue assessment (where the maximum stress range was calculated as twice the hot spot stresses; see Section 4.3.4), likely underpredicted the design life. To mitigate fatigue failure for the prototype, a design decision was made to specify full penetration, profiled welds where required. These welds added to the fabrication costs; more detailed fatigue analysis, and validation of structural loading via the prototype deployment, will be used to achieve a lower-cost fatigue solution in future design work.

Although Ershigs had withdrawn as the structural designer for the H2 WEC hull, they still anticipated designing the laminate for the mixed materials concept. While kicking off the test-supported mixed materials optimization phase of the Project, Ershigs' schedule precluded their involvement. As such, Glosten was engaged to design the laminate and Corrosion Companies Inc was engaged to fabricate the laminate for testing. Ershigs provided guidance on preferred fabrication methodology and fabricated one panel-type when CCI could not source the materials cost effectively.

Fabrication of the hand-laid, infused, and wound panels for test articles revealed a challenging aspect of FRP; thickness was variable, surfaces wavy, and even panels formed on flat tables had significant curve post-cure. In testing, the variability of coupon thickness was accounted for by measurement. For some tests, the curve present in the coupons induced some level of strain when they were installed in the load frame; these strain readings prior to loading were zeroed out per the test specification.

Seawater saturation was expected to adversely affect the adhesive bond of the DLS joints. While including seawater saturation simulation in testing the DLS specimens would have undoubtedly been informative, the schedule and budget did not support this. Instead, PSF's from DNVGL standards were applied to account for seawater degradation.

The time required for fatigue cycle testing of DLS specimens was an unknown quantity when the test plan was drafted. As testing progressed, it was evident that some of the planned load levels were not practical. Testing at load levels ranging from 10% to 90% of the ultimate load were planned. However, only one specimen was tested at 25% load, and none at 10%. The specimen tested at 25% load was cycled over 15 million times before being removed from the load frame intact. At a rate of 5 Hz (to keep the material from self-heating), this test took about 35 days. As such, the load levels were adjusted such that 31% load was the lowest used for testing-to-failure, and the number of tests performed at the lowest loads was

reduced. Instead, specimens were tested at intermediary load levels, yielding a smoother fatigue curve over a wide region of practical utility.

8 SYSTEM INTEGRATION AND FUTURE WORK

Under 6610, the H2 WEC hull was brought from concept design to final design with a complete structural drawing package. Under 7347 the final design was converted to fabrication drawings and accuracy was validated by using the fabrication drawing package to virtually build the WEC in a 3D SolidWorks computer aided design model.

The design methodology employed in this 6610 Project will be used in the development of the next-generation StingRAY (H3) WEC to be designed for deployment at PacWave-South in Oregon under newly awarded DE-EE0008954 (8954) Project. The mixed materials concept developed in this 6610 Project will be explored further in 8954 and incorporated to the degree that analysis indicates support for improved LCOE or other relevant metrics.

This 6610 Project used FRP components fabricated by CCI and Ershigs. C-Power will continue to develop relationships with these fabricators as the mixed materials design progresses and refines under the 8954 Project. As appropriate, they will be consulted for their expertise in FRP fabrication.

Adhesives from both ITT and Huntsman, tested in 6610 Project, satisfied design requirements. C-Power will continue to develop relationships with these suppliers. Practical considerations (e.g. cost) will likely influence C-Power decision as to which adhesive to select for H3 WEC design. Options for testing the adhesive's performance under seawater saturated conditions will be explored, and the results may be significant in adhesive selection.

The *System Integration Plan* covers plans for integration of Project improvements into C-Power's technology in more detail (see Appendix 11.15).

9 CONCLUSIONS

The 6610 Project objectives were to improve the AW PWR by 64% and DW PWR by 15%, and to decrease LCOE. This was achieved by decreasing CAPEX, reducing structural mass, and increasing energy production performance.

A generational advancement of the StingRAY H1 WEC hull structure was realized following 6610 Project initiation. This next-generation StingRAY H2 WEC hull architecture significantly increases power performance of the WEC, while reducing the complexity and cost of the WEC system through efficient use of structural and power generation components, along with simplified component geometries aimed at reducing manufacturing costs. One of the simplifications included the use of cylindrical structural elements. In consultation with DOE, it was agreed that these offered a more practical area of interest to explore, yielding a better use of available resources. Under 6610, the H2 WEC was progressed from concept to final design with structural drawings. The new design eschewed the costly steel ballast utilized by the Project Baseline WEC, in favor of low-cost concrete and sea water ballast.

A mixed materials approach to further structural optimization was validated with extensive laboratory structural testing. This approach substituted FRP for steel where appropriate, resulting in cost and weight savings. An adhesive, double lap shear joint was used to join the FRP and steel subcomponents. The benefits of steel were maintained where most useful, for instance at structural joints where the stiffness of steel was required and the complex geometry was more readily fabricated with steel. However, there are structural spans whose simple shapes are readily fabricated with mandrel-wound FRP and where significant cost and weight savings can be found. Multiple specimens of three different FRP panel types

were subjected to five different ASTM tests for a total of 166 tests. Guided by DNV GL standards, the test results were used to establish characteristic material values for the constituent layers of the FRP laminate, allowing the concept layup to be optimized for the design. A total of 85 full-scale sectioned adhesive joint specimens were fabricated using three candidate adhesives and multiple adhesive bond thicknesses and subjected to testing under fatigue and ultimate loading conditions. Two adhesive configurations tested met all established design requirements, validating the feasibility of the mixed materials design concept.

The 6610 Project SPA metric improvement goals were substantially surpassed, with improvements of 99.4 and 88.0% for AW and DW PWR, respectively. Although there was no specific goal established for LCOE improvement, the 54.1% reduction represented a resounding success for the Project.

Under the 8954 Project, the mixed materials concept developed in this 6610 Project will be explored in conjunction with further re-design and incorporated to the degree that analysis indicates support for improved LCOE or other relevant metrics.

10 REFERENCES

- [1] "Design requirements for marine energy systems," International Electrotechnical Commission, IEC 62600-2, Ed. 1, Aug. 2016.
- [2] "StingRAY Failure Mode, Effects and Criticality Analysis," Columbia Power Technologies, S1-FMECA-1000 v3.0, Sep. 2014.
- [3] "Design of Offshore Steel Structures," DNV, DNV-OS-C101, Apr. 2011.
- [4] "Buckling Strength of Shells," DNV, DNV-RP-C202, Jan. 2013.
- [5] "Rules for Classification of Ships," DNV, 2017.
- [6] "Fatigue Design of Offshore Steel Structures," DNV, DNV-RP-C203, 2014.
- [7] "Direct Analysis of Ship Structures," DNV, CN 34.1, 2009.
- [8] "Position Mooring," DNV, DNV-OS-E301, Oct. 2010.
- [9] "Recommended Practice for Planning, Designing and Constructing Fixed Offshore Platforms - Working Stress Design," API, API RP 2A, 2014.
- [10] "Sea Transport Operations," DNV, DNV-OS-H202, 2015.
- [11] "Composite Components," DNV GL, DNVGL-ST-C501, Aug. 2017.
- [12] M. Y. Tsai, D. W. Oplinger, and J. Morton, "Improved Theoretical Solutions for Adhesive Lap Joints," *Int J Solids Struct.*, vol. 35, no. 12, pp. 1163–1185, 1998.
- [13] S. Spencer (Ershigs), email to P. Lenee-Bluhm, "Re: CPT WEC testing," 01-Oct-2019.
- [14] T. Post (ITW), email to P. Lenee-Bluhm, "Re: Plexus MA 560 cost," 23-Aug-2019.
- [15] A. Mansfield (Huntsman), email to P. Lenee-Bluhm, "Re: Columbia Power Technologies 08292019 (1)," 29-Aug-2019.
- [16] "Standardized Cost and Performance Reporting for Marine and Hydrokinetic Technologies," US Dept of Energy, <http://en.openei.org/community/document/mhk-lcoe-reporting-guidance-draft>, Oct. 2015.

11 APPENDICES [PROTECTED DATA]

11.1 Appendix: Design Load Cases for Structural Optimization

DE-EE0006610 M2.1 Design Load Cases for Structural Optimization v2.0 PD 07-15-2016.pdf

11.2 Appendix: Metocean Report

DE-EE0006610 M2.1.2 Metocean Report S1-DB-01 v4.1 PD 06-05-2015.pdf

11.3 Appendix: StingRAY Design Loads

DE-EE0006610 M2.2.1 StingRAY Design Loads v2.1 PD 03-19-2018.pdf

11.4 Appendix: CPower WEC Design Documentation

DE-EE0006610 M2.2.2 18024 CPT WEC Design Documentation Rev-A PD 10-31-2018.pdf

11.5 Appendix: CPower WEC Structural Arrangement

DE-EE0006610 M2.2.3 18024-100-01 WEC Structure Rev-B PD 04-26-2019.pdf

11.6 Appendix: Summary of Component Design Report

DE-EE0006610 M6.1c Summary of Component Design Report PD v1.0 11-26-2019.pdf

11.7 Appendix: Test Article Design Technical Memo

DE-EE0006610 M4.1 18024.01-200-01 Test Article Design Technical Memo Rev.A PD 10-31-2018.pdf

11.8 Appendix: Composite Test Program Memo

DE-EE0006610 M3.5.1 18024.01-200-02 Composite Test Program Memo Rev.A PD 10-31-2018.pdf

11.9 Appendix: WEC Design Alternative Composites Coupon Panels

DE-EE0006610 M3.5.2 18024-100-20 WEC Design Alternative Composites Test Program Rev.B PD 10-31-2018.pdf

11.10 Appendix: CPower Coupon and Double Lap Shear Specimen Test Report (public data)

DE-EE0006610 M5.3 Coupon and DLS Specimen Test Report revA UD 09-16-2019.pdf

11.11 Appendix: Optimization Memo

DE-EE0006610 M5.5 Optimization Assessment Memo PD v1.1 10-31-2019.pdf

11.12 Appendix: SPA and LCOE Impact Assessment

DE-EE0006610 M6.1b SPA and LCOE Impact Assessment PD v1.0 11-05-2019.pdf

11.13 Appendix: Energy Production Assessment for DOE LCOE and SPA Reporting

DE-EE0006610 M6.1b.3 Energy Production Assessment for DOE LCOE and SPA Reporting v1.0 PD 10-14-2019.pdf

11.14 Appendix: Baseline and Final TAEP Calculations

DE-EE0006610 M6.1b.4 Baseline and Final TAEP Calculations v1.0 PD 10-14-2019.pdf

11.15 Appendix: System Integration Plan

DE-EE0006610 M6.1a System Integration Plan PD v1.0 11-26-2019.pdf